Growth Rates of the Deceleration-Phase Rayleigh–Taylor Instability

V. LOBATCHEV, M. UMANSKY, and R. BETTI

University of Rochester
Laboratory for Laser Energetics

UR LLE

Growth Rates of the Deceleration-Phase Rayleigh–Taylor Instability

V. Lobatchev, M. Umansky, and R. Betti

Laboratory for Laser Energetics, U. of Rochester

The evolution of inner-surface perturbations during the deceleration phase of a planar foil and a spherical shell is studied by using high-resolution, two-dimensional Eulerian simulations, and the results are compared with a theoretical model for the growth rates. The planar simulations concern the deceleration of a foil compressing a low-density shocked material against a rigid wall. The two-dimensional spherical simulations concern direct-drive NIF capsules. The output of the one-dimensional code *LILAC* at the beginning of the deceleration phase with an imposed inner-surface perturbation is used as the input of the two-dimensional simulations. It is found that the simulated growth rates are significantly lower than their classical values. In addition to the finite density-gradient scale length, further stabilization is provided by mass ablation off the inner surface of the shell. This work was supported by the U.S. Department of Energy Office of Inertial Confinement Fusion under Cooperative Agreement No. DE-FC03-92SF19460.

The deceleration-phase instability occurs in the final phase of the implosion

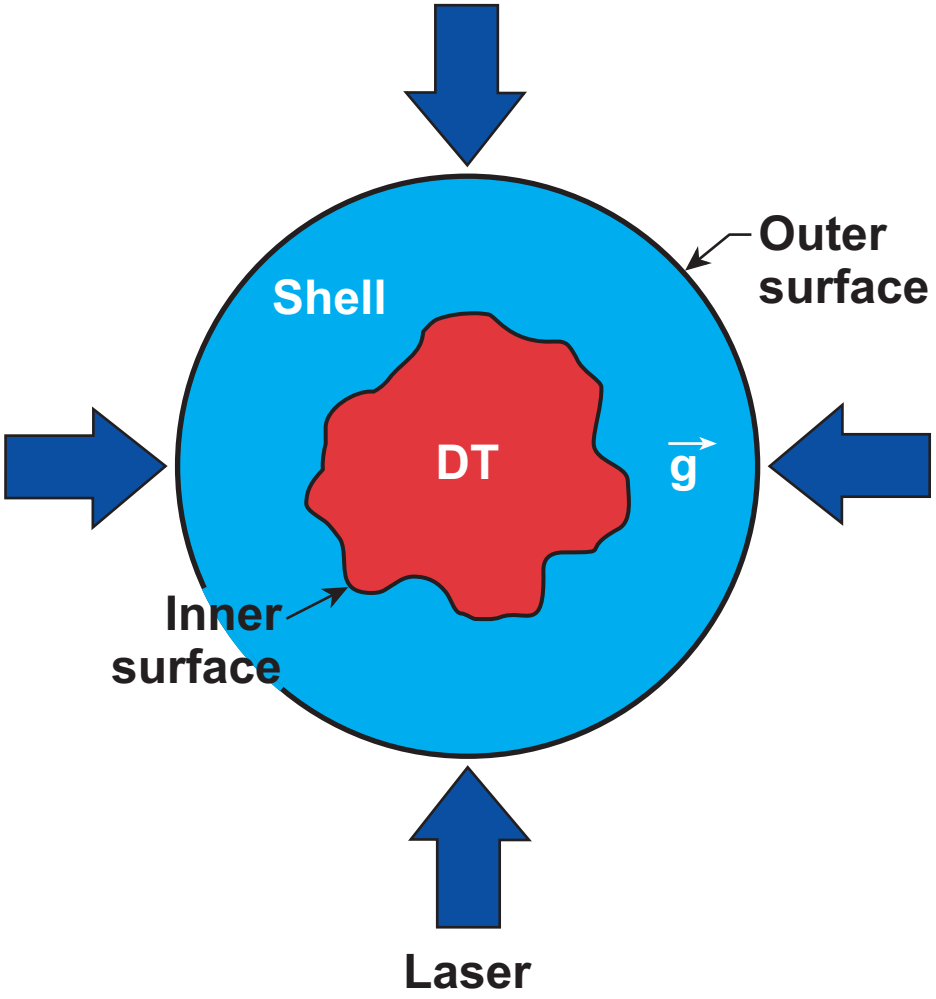

During the deceleration phase, the inner surface of the shell is RT unstable and its perturbations grow exponentially.

What is investigated?

UR LLE

- Mass ablation
- Density-gradient scale length
- Inner-surface acceleration

} Important in the RT instability

- Reduction of the deceleration-phase Rayleigh–Taylor instability
- Both planar and spherical numerical simulations were carried out to study all of the above.

Eulerian code was developed to simulate the deceleration-phase instability

UR LLE

- Standard gas dynamic equations
- Heat transfer
- Local α-particle deposition
- To speed up the heat transfer calculation, the simulations were done with an Eulerian code.

Impulsive deceleration by a series of shocks is followed by continuous deceleration

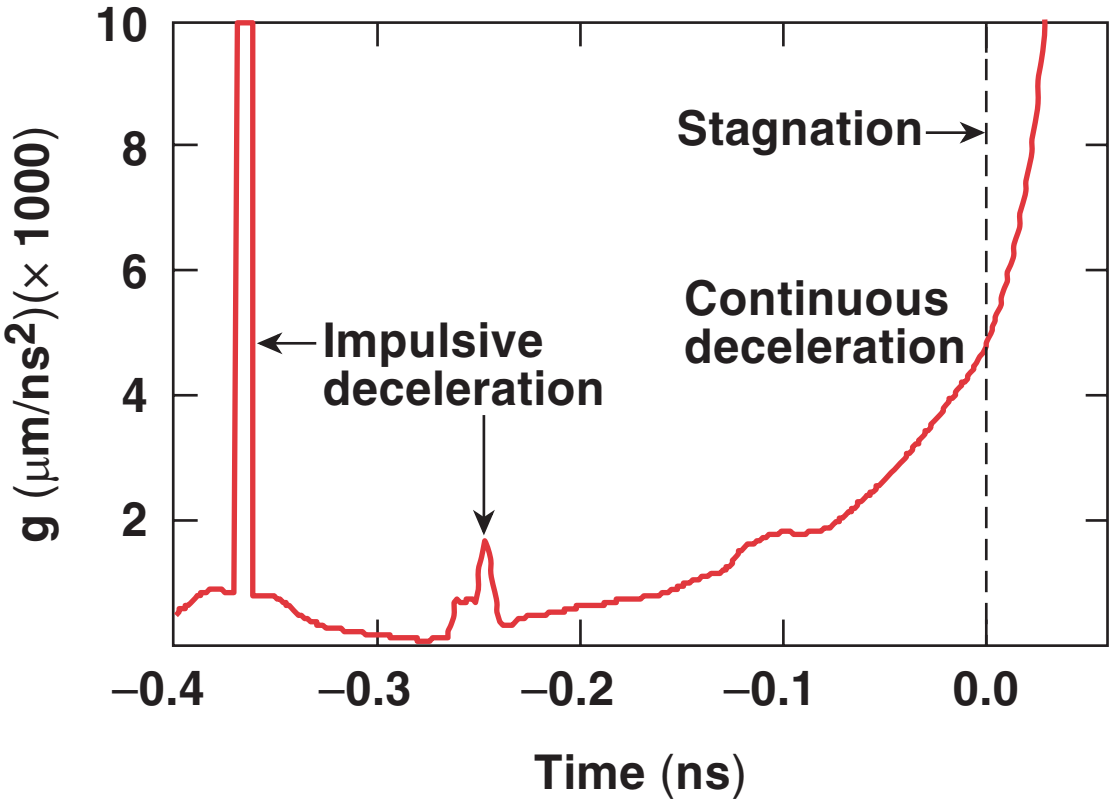

- Why does the deceleration behave in this manner?
- What do we call the deceleration phase?
- Growth rate?

The decelerating foil problem provides the basic understanding of the deceleration-phase instability

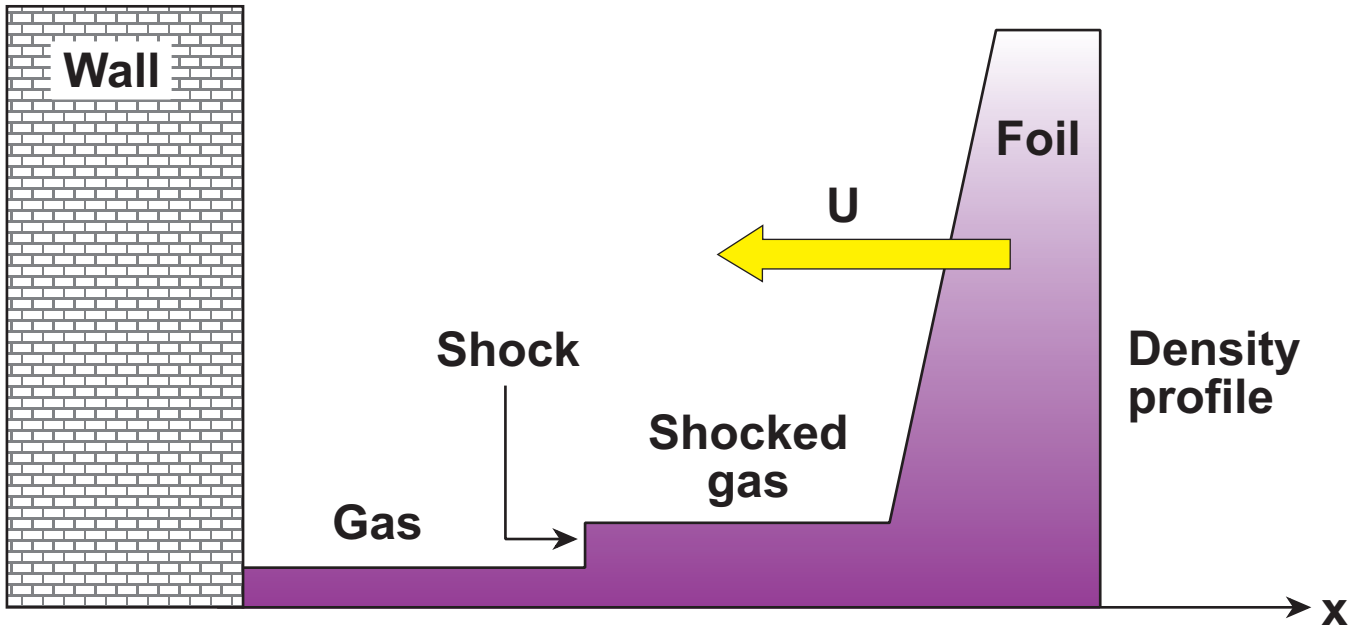

- The shock reflected from the wall slows down the foil, which in turn compresses the gas and decelerates.
- The 1-D problem can be solved analytically leading to a clear understanding of the relevant physics issues.

The foil is slowed down both impulsively and continuously

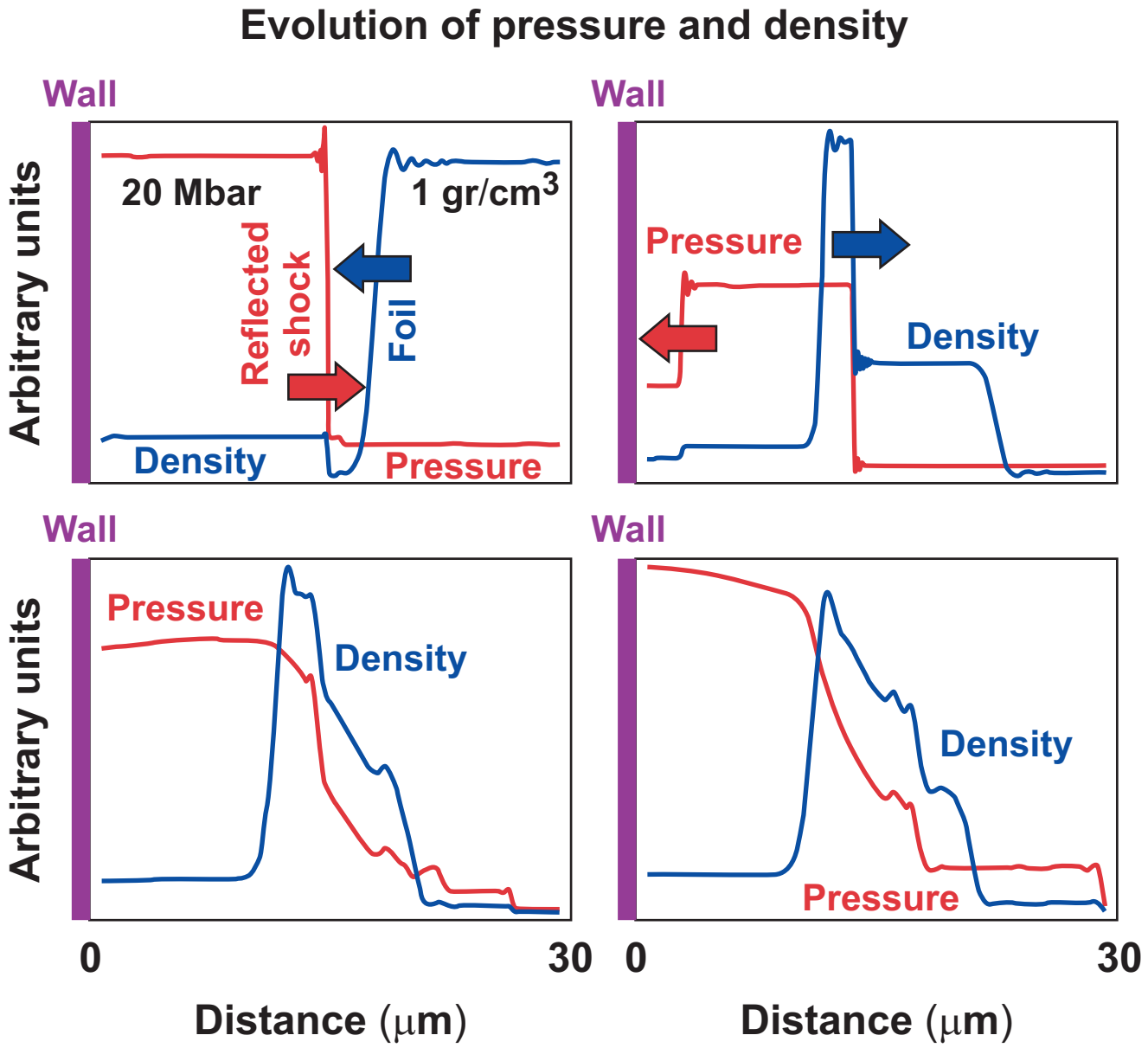

TC5392

What physical mechanism is responsible for the mass ablation at the shell's surface?

- The shell is much colder than the hot spot.
- The heat flux leaving the hot spot is deposited on the shell surface.
- Expansion of the heated material causes the mass ablation from the shell into the hot-spot.

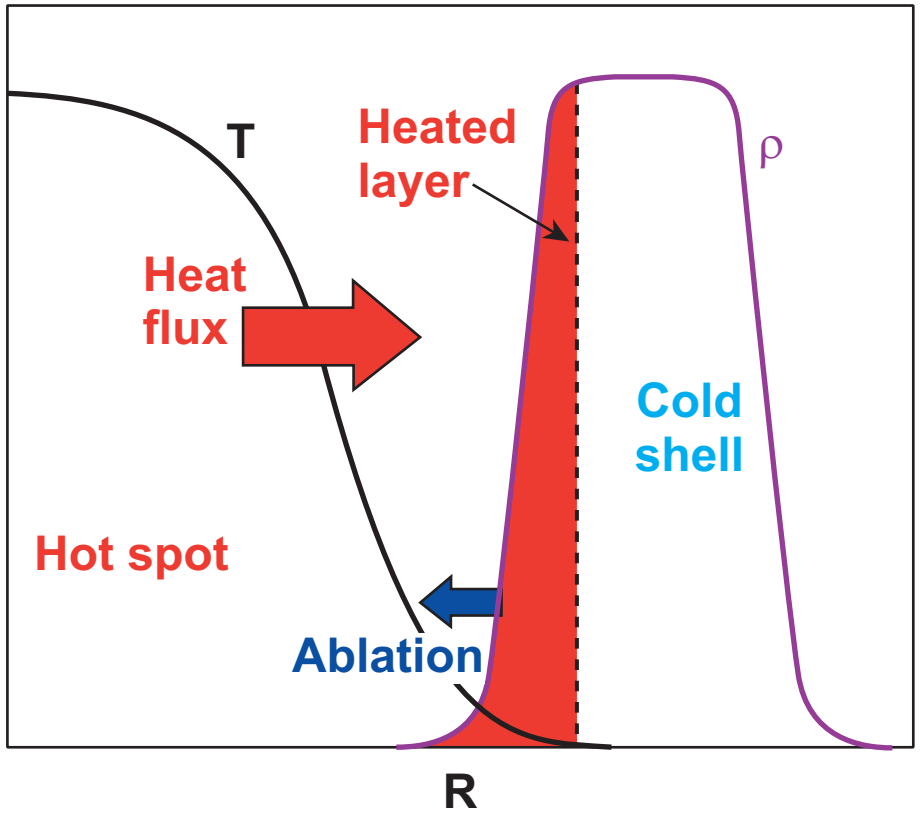

Spherical simulations were performed to determine the growth rates during the deceleration phase

UR LLE

- 1-D *LILAC* output for a typical NIF target was used for the initial density, pressure, and velocity distribution.
- A 1-D Eulerian simulation is performed until the beginning of the continuous deceleration phase.
- The 2-D pertubations of the shell's inner surface are introduced ~200 ps before the stagnation begins.
- A Fourier transform is used to determine the amplitude of each mode.
- The growth rates are determined by fitting the time history of each mode.

High-resolution simulations are required to resolve short-wavelength modes with $k > 1/L_m$

UR LLE

$$L_m = \min_x \left(\frac{1}{\rho} \frac{d\rho}{dx} \right)^{-1}$$

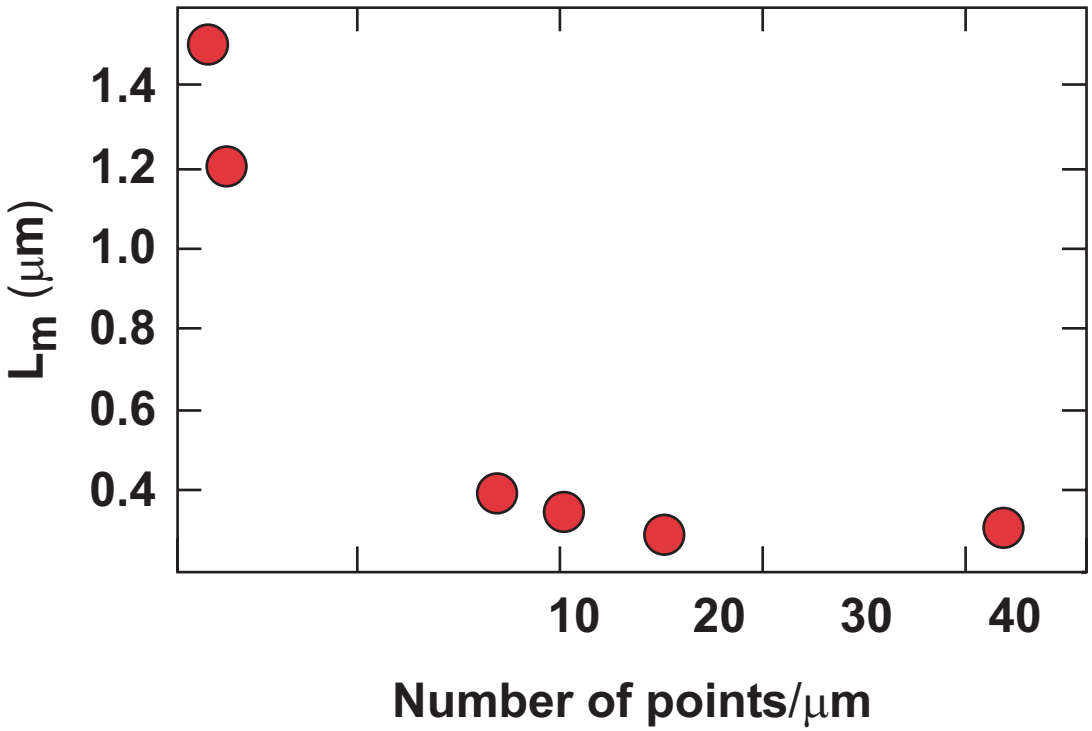

- L_m obtained in 1-D numerical simulations depends on resolution.
- L_m does not decrease dignificantly when the grid refinement is $\Delta x < 0.05$ μm.

TC5571

The minimum density-gradient scale length is ~1μm

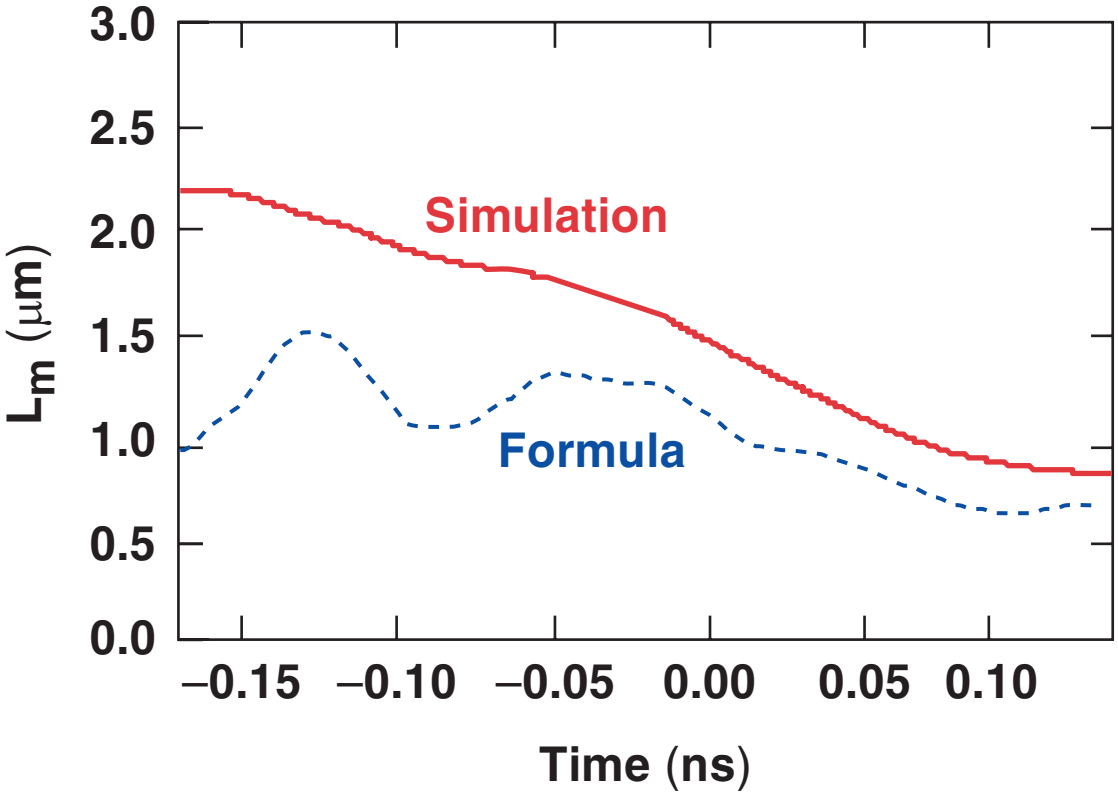

$$L_m = \min_r \left(\frac{1}{\rho} \frac{\partial \rho}{\partial x} \right)^{-1} \qquad L_m = 6.8 R_{hs} \left(\frac{m_i P_{hs}(t)}{2 \rho_{shell} T_{hs}(0,t)} \right)^{5/2}$$

TC5572

Ablation velocities obtained from both theory and simulation are of the order of 20 μm/ns

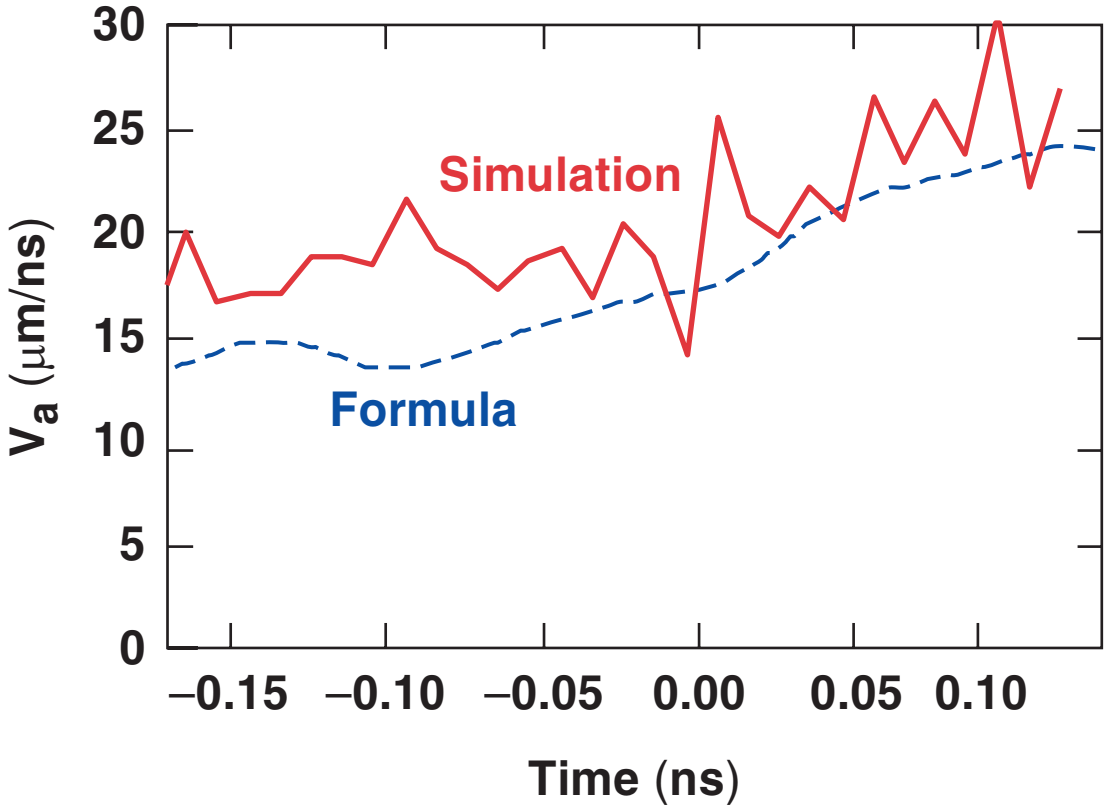

$$V_a\left(\frac{\mu m}{ns}\right) = 1.2 \cdot 10^3 \frac{T_{hs}^{5/2}(keV)}{R_{hs}(\mu m)\rho_{shell}\left(\frac{g}{cm^3}\right)}$$

TC5573

Growth rates of the deceleration-phase instability for the planar foil are reduced by mass ablation

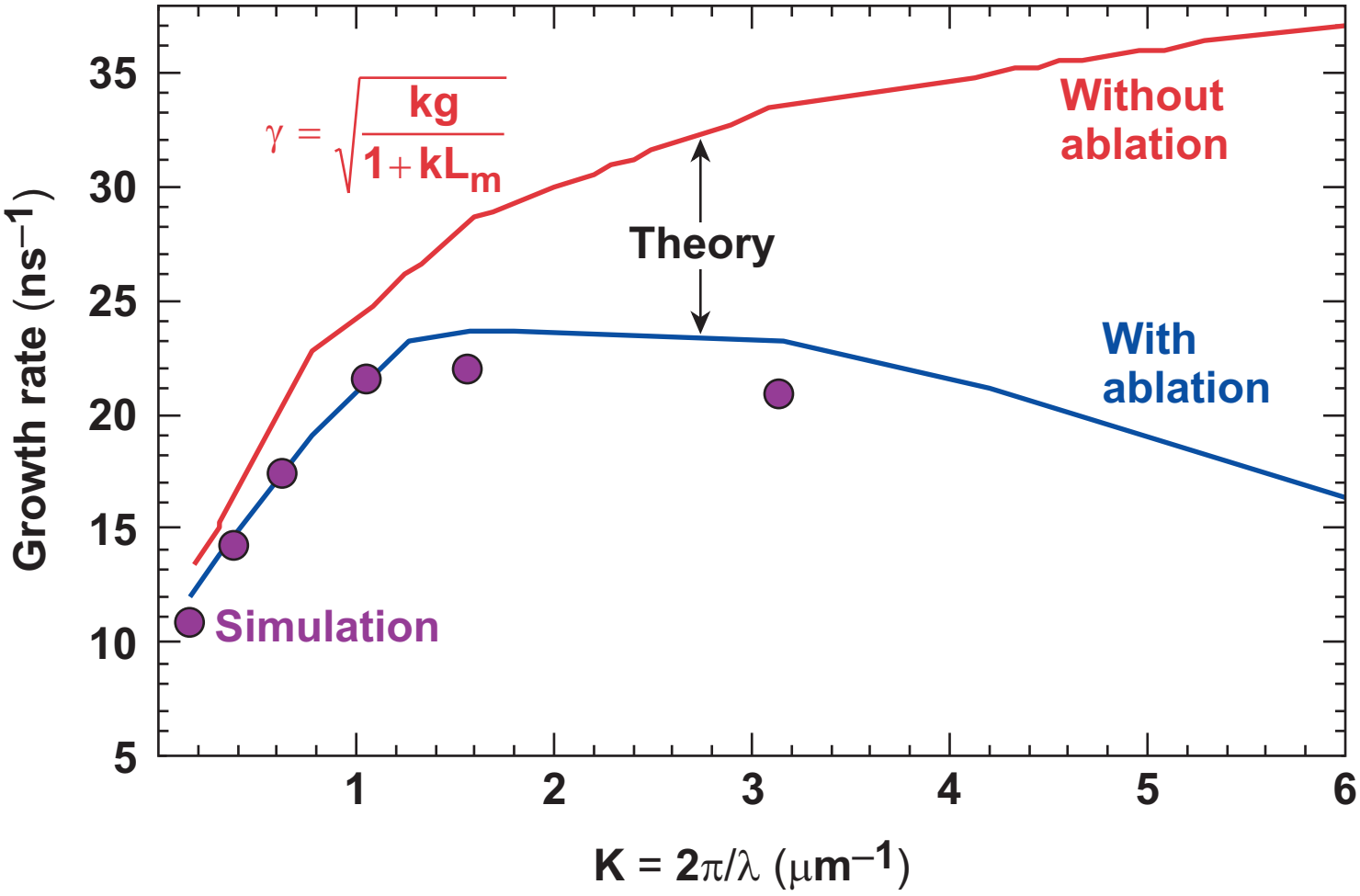

TC5366a

Results of 2-D spherical simulations of a NIF-like capsule confirm the importance of mass ablation

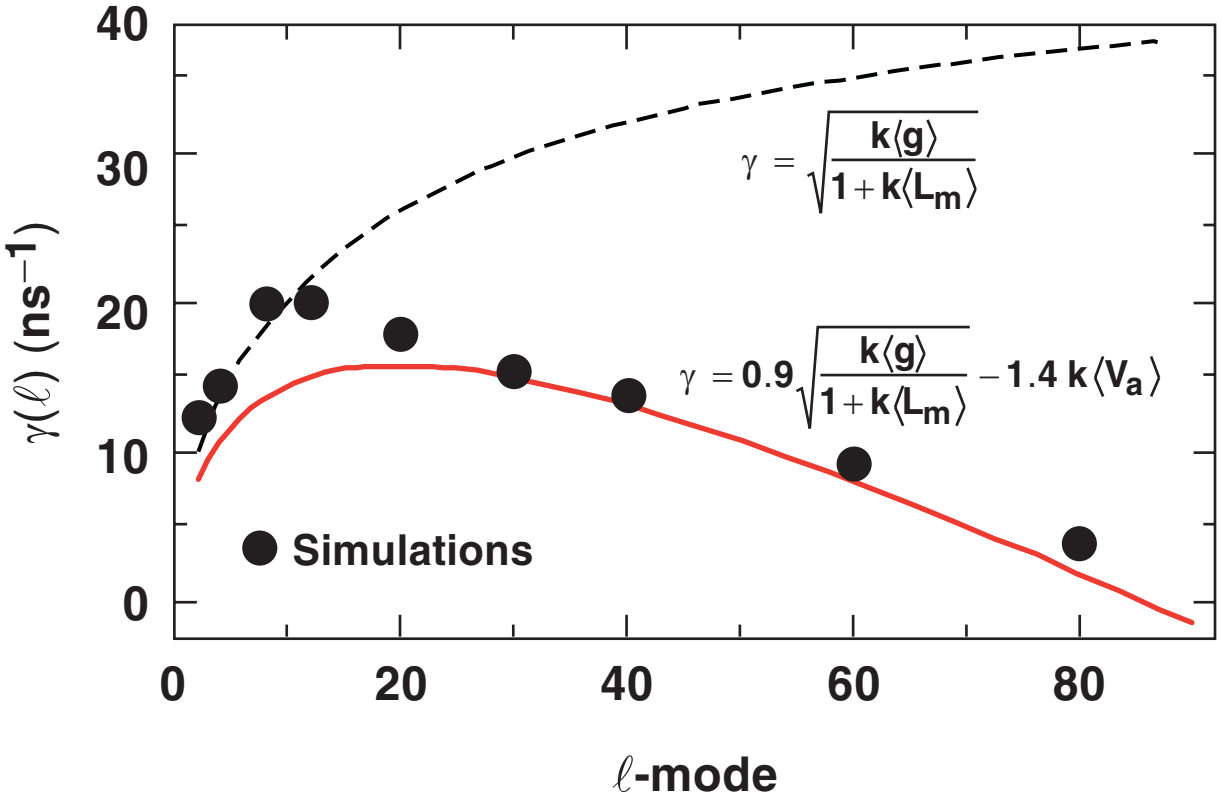

- The cutoff is observed at ℓ = 90 in the instability spectrum. All modes with ℓ > 90 are stable.

Conclusions

UR LLE

- Two stages of the deceleration-phase instability are observed: deceleration by a series of shocks and continuous deceleration.
- Mass ablation through the inner surface and finite density-gradient scale length are the main stabilizing factors during the RT growth.
- The significant reduction in the RT instability growth rate is observed due to the mass ablation. The spectrum of the deceleration-phase instability exhibits a cutoff for mode numbers of about $\ell = 90$.
- For $\ell \sim 50$, the calculated growth rate is less by a factor of 3 than the conventional estimate, neglecting ablation.

Planar Model

Planar simulations reproduce the behavior of ICF capsule implosions

UR LLE

- Hot-spot temperature and radius and peak shell density have the same order of magnitude in planar and spherical cases.

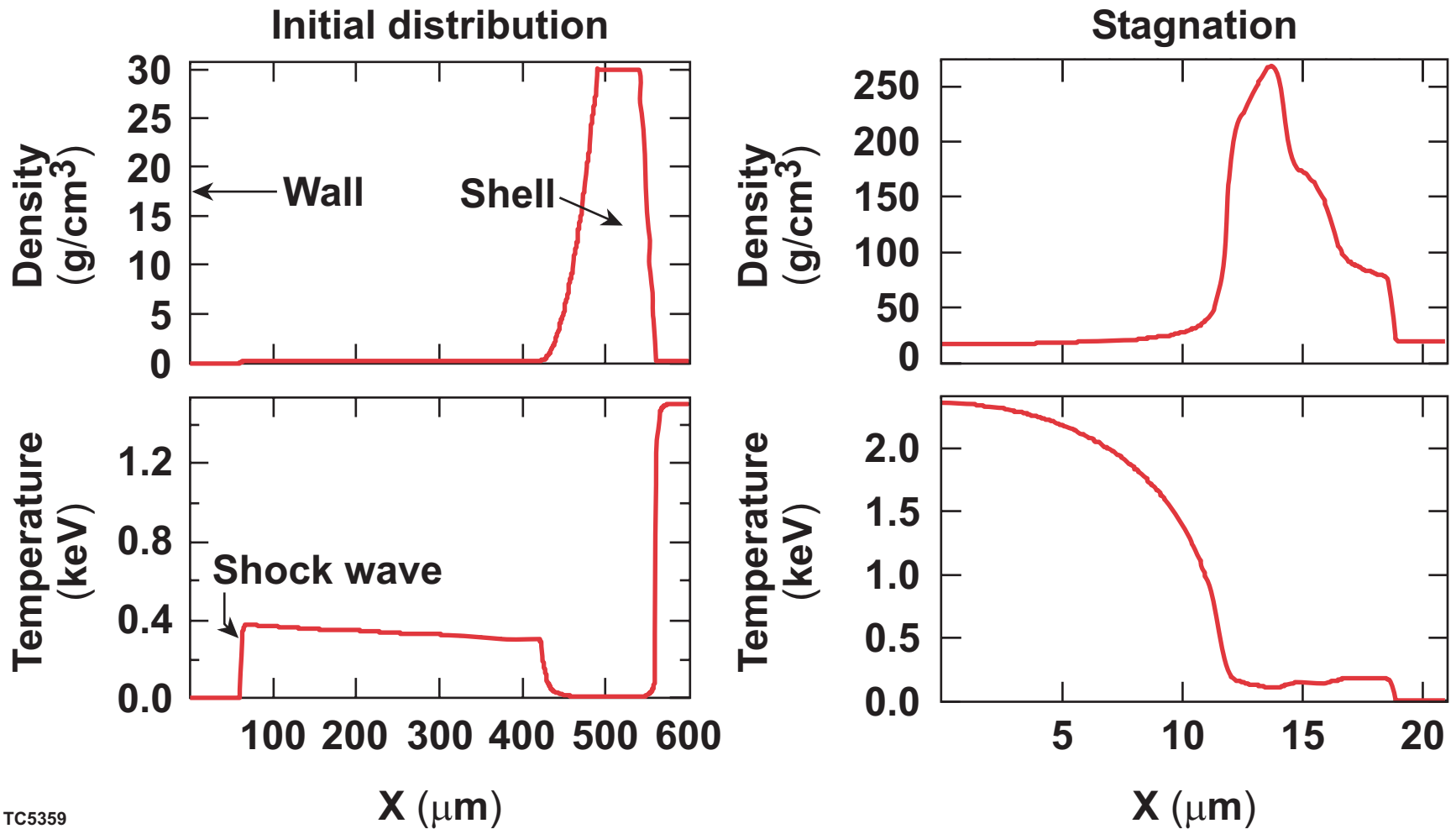

TC5359

The density-gradient scale length is small

- **Balance of heat flux to the shell and internal energy flux leaving the shell**

$$pV_a \approx -\kappa(T_{sh})\frac{dT_{sh}}{dr} \approx \kappa(T_{sh})T_{sh}\,\frac{1}{\rho_{sh}}\frac{d\rho_{sh}}{dr}$$

- **The density-gradient scale length is found using the formula for the ablation velocity:**

$$L_m = \left[\frac{1}{\rho}\frac{d\rho}{dr}\right]^{-1}_{min} \approx 1.6\,\frac{M_i\kappa(T_{sh})}{\rho_{sh}V_a} = 8R_{hot\text{-}spot}\left(\frac{T_{shell}}{T_0}\right)^{5/2}$$

- **For NIF: $L_m \sim 1\ \mu m$**

The ablation velocity is determined from the energy balance

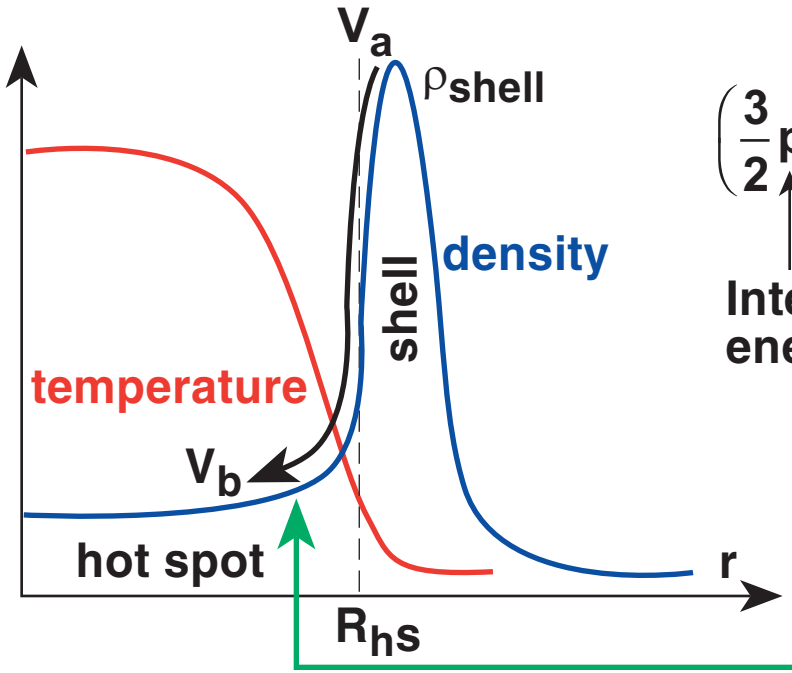

$$\left(\frac{3}{2}p_bV_b + p_bV_b\right) = \kappa_{Spitz}(T_b)\frac{dT_b}{dR_{hs}}$$

Internal energy flux

pdV work rate

Energy flux balance

- Hot-spot temperature profile: $T_{hs} = T_0\left(1-\frac{r^2}{R_{hs}^2}\right)^{2/5}$
- Use the EOS: $p_bV_b = 2\rho_bV_bT_b / M_i = 2\dot{m}T_b / M_i$
- Ablation velocity: $V_a = \frac{\dot{m}}{\rho_{shell}} = 0.2\frac{M_i\kappa_{Spitz}(T_0)}{\rho_{shell}R_{hot\ spot}}$

The deceleration-phase instability consists of a RM phase and a RT phase

UR LLE

- Linear RM instability is observed when shocks are coming.
- Exponential RT instability is seen during the continuous deceleration stage.

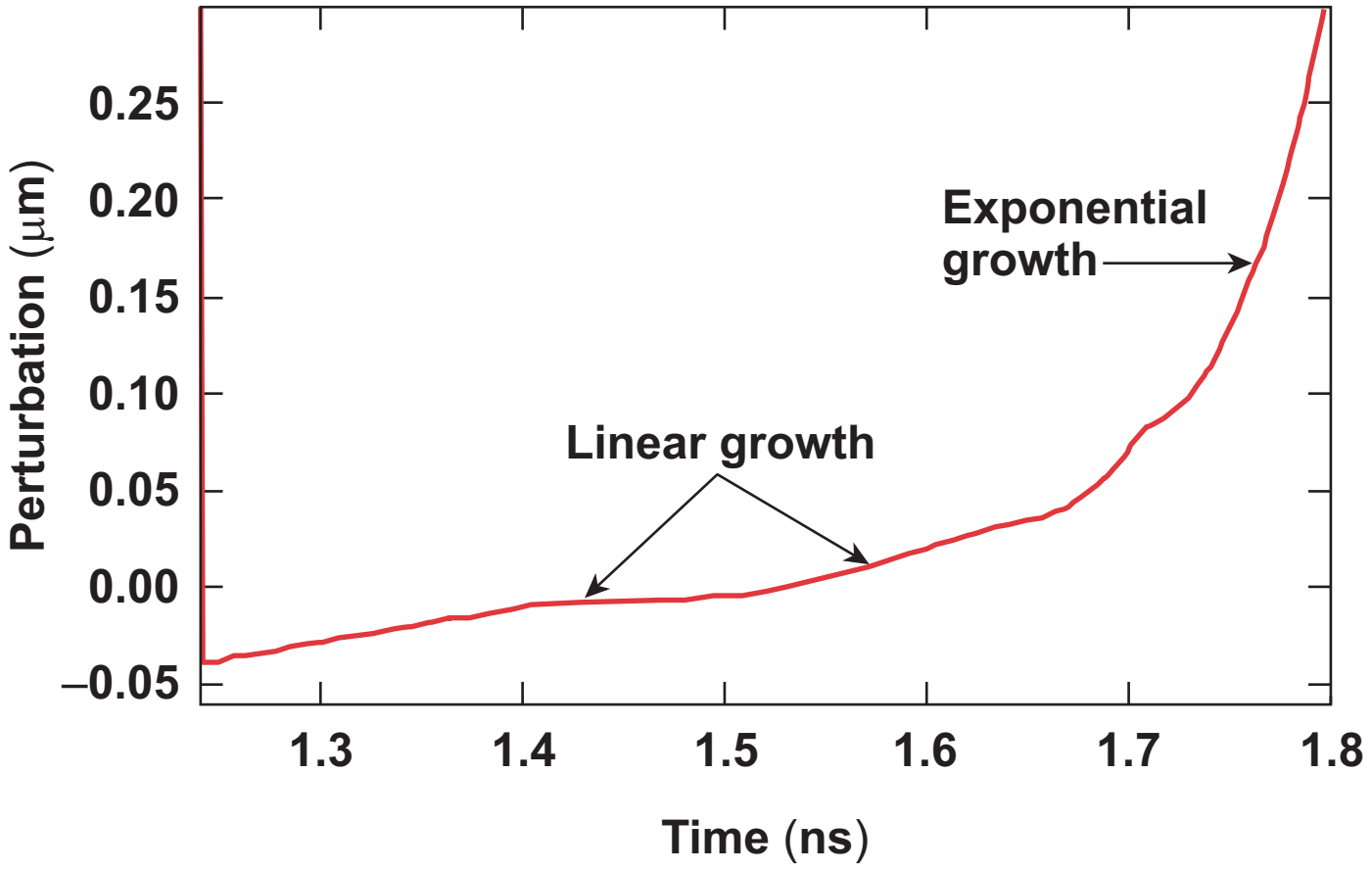

TC5363

Finite density-gradient scale length and mass ablation have the largest stabilizing effect

- Simple models include only $d^2\eta/dt^2 = kg\eta$, compressibility, ablation, and L_m.

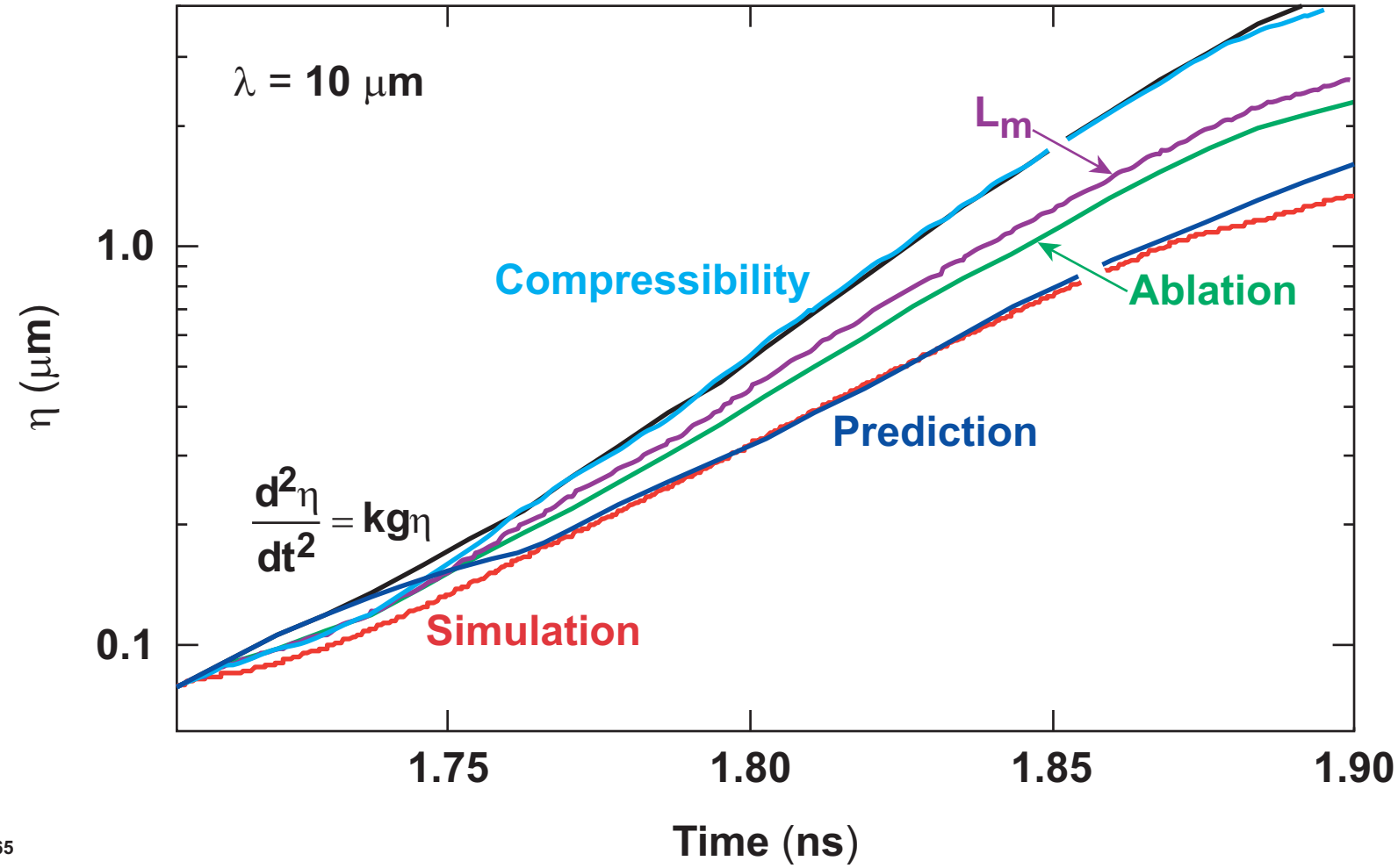

TC5365